

Supplementary Information

Towards the design of effective multipodal contacts for use in the construction of Langmuir-Blodgett films and molecular junctions

Enrique Escorihuela,^{a,b} Pilar Cea,^{a,b,c,*} Sören Bock,^d David C. Milan,^e Saman Naghibi,^e Henry M. Osorio,^f Richard J. Nichols,^{e,*} Paul J. Low,^{d,*} Santiago Martin.^{a,b,*}

^a Departamento de Química Física, Facultad de Ciencias, Universidad de Zaragoza, 50009, Spain.

^b Instituto de Ciencias de Materiales de Aragón (ICMA), Universidad de Zaragoza- CSIC, 50009 Zaragoza, Spain.

^c Instituto de Nanociencia de Aragón (INA), edificio i+d Campus Rio Ebro, Universidad de Zaragoza, C/Mariano Esquillor, s/n, 50018 Zaragoza, Spain and Laboratorio de Microscopías Avanzadas (LMA), Universidad de Zaragoza, 50018 Zaragoza, Spain.

^d School of Molecular Sciences, University of Western Australia, 35 Stirling Highway, Crawley, WA, 6009, Australia.

^e Department of Chemistry, University of Liverpool, Liverpool, L69 7ZD, United Kingdom

^f Departamento de Física, Escuela Politécnica Nacional, Av. Ladrón de Guevara, E11-253, 170525 Quito, Ecuador

AFM image for a LB film of 1 transferred to a gold substrate at 8 mN·m⁻¹

Figure S1 shows an AFM image for a LB film of **1** transferred to a gold substrate at 8 mN·m⁻¹. The image shows a uniform monolayer LB film largely free of perforations or holes and 3-dimensional defects.

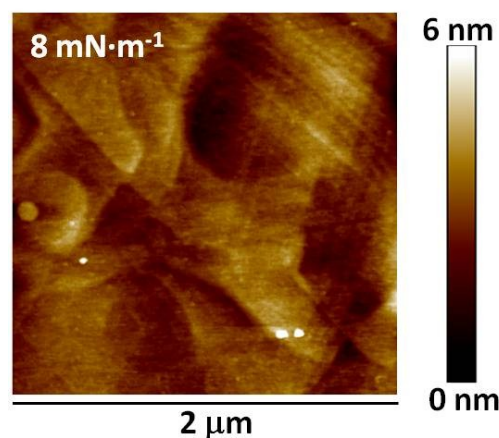


Figure S1. AFM image of a LB film transferred at 8 mN·m⁻¹ to a gold substrate.

LB film surface coverage

A bearing analysis of the AFM image showed in Figure 4 at $8 \text{ mN}\cdot\text{m}^{-1}$ (for mica substrates) was made in order to calculate the LB film surface coverage. In this analysis, the depths of all pixels of the image with respect to a reference point, i.e., the highest pixels, are analysed. This kind of analysis renders an accurate estimation of the percentage of area covered by the LB film, i.e. surface coverage, at every pixel depth. The analysis of a coverage data recorded over $2 \times 2 \mu\text{m}^2$ area indicates an average LB film-coverage of ca. 95.8%, Figure S2; that is, 4.2% of the gold substrate is not covered by the LB film. It is necessary to indicate here that for a LB film of **1** transferred to a gold substrate at $8 \text{ mN}\cdot\text{m}^{-1}$ the AFM image (Figure S1) does not show practically any perforation, holes or 3-dimensional defects, that is, a higher area covered by the LB film is obtained.

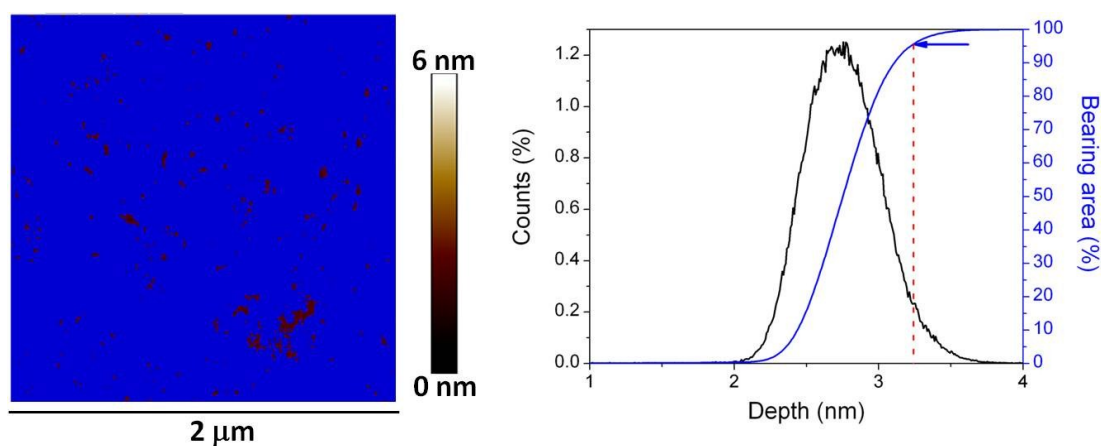


Figure S2. (Left): AFM image of an LB film of **1** transferred to a mica substrate at $8 \text{ mN}\cdot\text{m}^{-1}$ with the mask in blue indicating LB film-covered areas. (Right): Depth histogram showing the distribution of height data at different depth referred to a reference point, i.e. the highest pixel (black line). The blue line (bearing analysis) indicates the relative projected area covered at each depth value depicted as a blue mask in the topographic image. The red dashed vertical line accounts for the selected height threshold corresponding to the lowest maximum peak associated to the bare mica.

Preparation of gold nanoparticles (NPs) and Au@SiO₂ (SHINERS) NPs

The preparation of gold nanoparticles coated with an ultrathin silica shell involved two main steps ^{2,3} and they were prepared by the literature method.⁴⁻⁶

SHINERS NPs were characterised using Cyclic Voltammetry (CV) and Raman spectroscopy. To check the formation of silicate layer on gold nanoparticles, one drop

of SHINERS NPs were dried on glassy carbon electrode and a CV was recorded in diluted H_2SO_4 and no oxidation and reduction for gold was observed since the silicate layer effectively protects the gold nanoparticles.

Shell-isolated nanoparticle-enhanced Raman spectroscopy (SHINERS)

Figure S3 shows a Raman spectrum (RENISHAW inVia Raman Microscope at 532 nm laser excitation wavelength and with an exposure time of 10 s) for a LB film of **1** on Au(111) using SHINERS. The sharp band at 700 cm^{-1} is a vibrational mode attributed to molecule **1**. The band at 700 cm^{-1} is assigned to $\nu(\text{CH}_3\text{-S})$ by comparison with literature compounds. The band at 920 cm^{-1} is a trigonal ring breathing mode of the pyridyl group. Most importantly, the band at 400 cm^{-1} is assigned to $\nu(\text{Au-S})$ (ca. 400 cm^{-1}) of the thiomethyl anchoring moiety (see below for a discussion of the spectra for the control compound, (methylsulfanyl)benzene, which confirms this assignment).

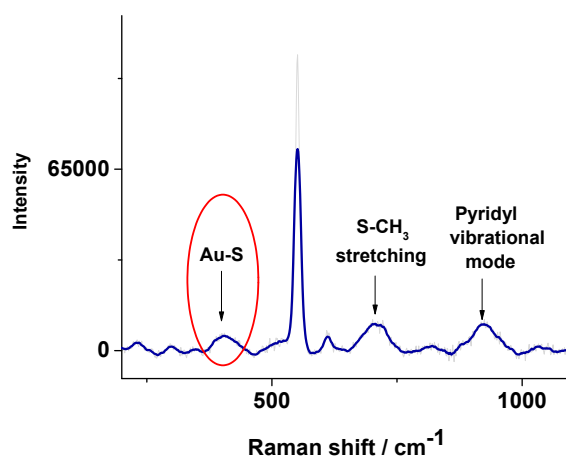
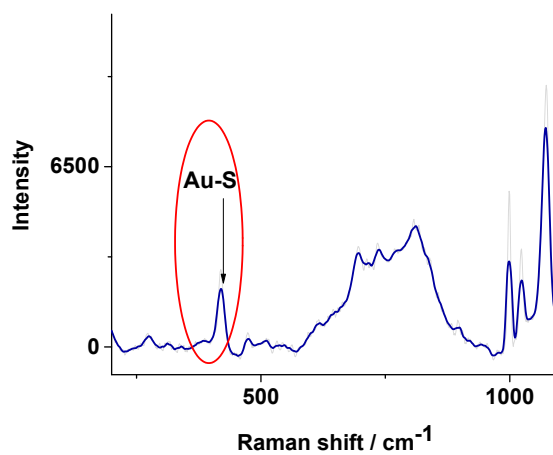


Figure S3. Raman spectrum of a LB films of **1** on Au(111) using shell-isolated nanoparticle-enhanced Raman spectroscopy (SHINERS).

To aid in these assignments, a self-assembled monolayer of the control compound (methylsulfanyl)benzene on gold was prepared and the Raman spectrum recorded using SHINERS (Figure S4a). The spectrum shows characteristic peaks attributed to (methylsulfanyl)benzene and a new the peak at ca. 380 cm^{-1} which is tentatively attributed to the $\nu(\text{Au-S})$ mode of the thiomethyl anchoring moiety.^{7, 8} To confirm this, a few drops of (methylsulfanyl)benzene were added onto a glass substrate. In this case, the SHINERS spectrum (Figure S4b) shows the characteristic peaks due to

(methylsulfanyl)benzene, but not the band at ca. 380 cm^{-1} (Figure S4b), consistent with its assignment to the $\nu(\text{Au-S})$ mode of a thiomethyl moiety anchored to gold.^{7, 8}

a)



b)

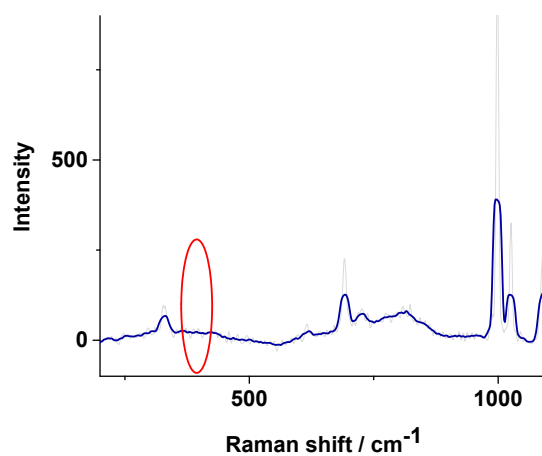


Figure S4. a) Raman spectrum of (methylsulfanyl)benzene on Au(111) using shell-isolated nanoparticle-enhanced Raman spectroscopy (SHINERS). b) Raman spectrum of (methylsulfanyl)benzene on a glass slide.

Proposed model of contact for compound 1 and similar pyridine-2,6-diyldi(methanethiol) compound

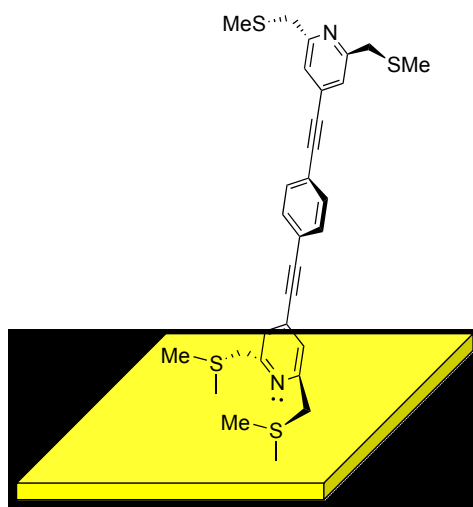


Figure S5. A sketch of molecule **1** (when forming a LB film) depicting the interaction with a gold substrate through two methylthio-ether groups and through the pyridine group.

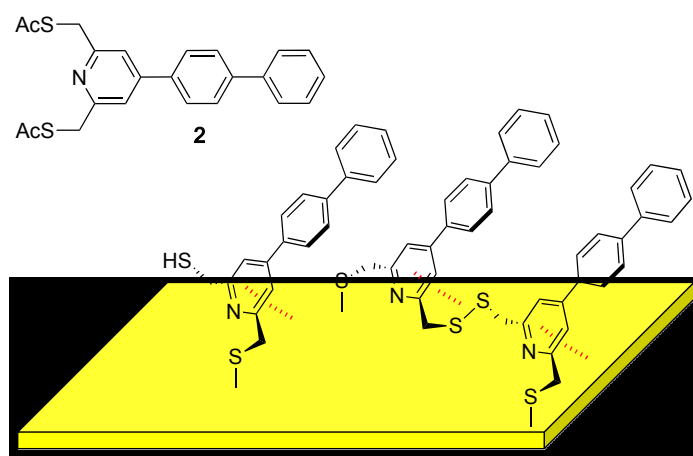


Figure S6. The thiol(ate) buttressed compound **2** (as the acyl protected derivative) and sketches depicting the variety of binding modes on gold described by Mayor, Zharnikov and colleagues.¹

Determination of the LB film thickness by using a height profile in an AFM image

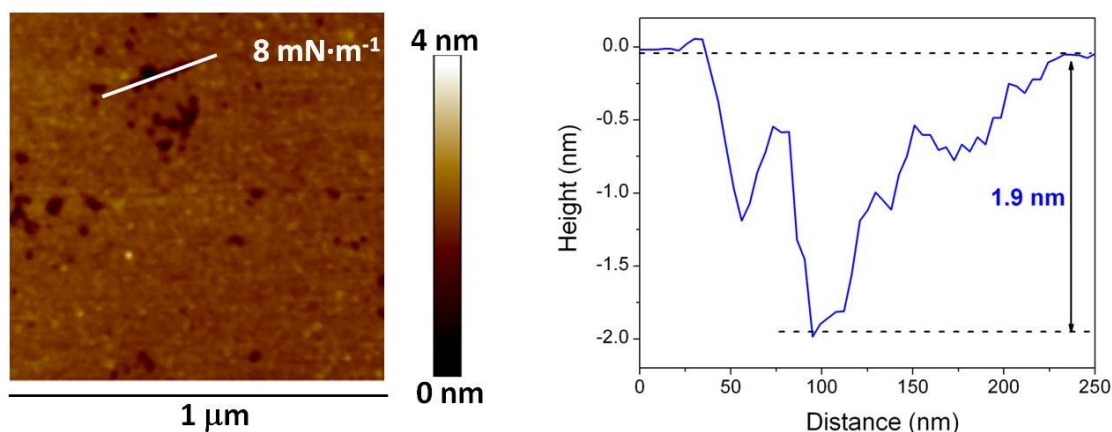


Figure S7. An AFM image of a LB film of **1** deposited onto mica at $8 \text{ mN}\cdot\text{m}^{-1}$. The thickness of the LB film was obtained measuring the height profile using a defect on the monolayer as illustrated.

References

1. F. Sander, J. P. Hermes, M. Mayor, H. Hamoudi and M. Zharnikov, *Phys. Chem. Chem. Phys.*, 2013, **15**, 2836-2846.
2. J. F. Li, X. D. Tian, S. B. Li, J. R. Anema, Z. L. Yang, Y. Ding, Y. F. Wu, Y. M. Zeng, Q. Z. Chen, B. Ren, Z. L. Wang and Z. Q. Tian, *Nat. Protoc.*, 2013, **8**, 52-65.
3. J. F. Li, Y. F. Huang, Y. Ding, Z. L. Yang, S. B. Li, X. S. Zhou, F. R. Fan, W. Zhang, Z. Y. Zhou, D. Y. Wu, B. Ren, Z. L. Wang and Z. Q. Tian, *Nature*, 2010, **464**, 392-395.
4. G. Frens, *Nature-Phys. Sci.*, 1973, **241**, 20-22.
5. J. F. Li, A. Rudnev, Y. C. Fu, N. Bodappa and T. Wandlowski, *ACS Nano*, 2013, **7**, 8940-8952.
6. T. A. Galloway, L. Cabo-Fernandez, I. M. Aldous, F. Braga and L. J. Hardwick, *Faraday Discuss.*, 2017, **205**, 469-490.
7. W. J. Balfour, K. S. Chandrasekhar and S. P. Kyca, *Spectrochim. Acta A*, 1986, **42**, 39-42.
8. M. X. Liu, B. B. Xie, M. J. Li, Y. Y. Zhao, K. M. Pei, H. G. Wang and X. M. Zheng, *J. Raman Spectrosc.*, 2013, **44**, 440-446.